The Third International Symposium on Optimization and Systems Biology (OSB'09)
Zhangjiajie, China, September 20–22, 2009

Mathematical Modeling of Signaling Pathways Leading to Type I IFN Gene Expression

Xiufen Zou[1,*] Xueshuang Xiang[1] Yan Chen[2] Zishu Pan[2]

[1] School of Mathematics and Statistics, Wuhan University, Wuhan, 430072, China
[2] College of Life Sciences, Wuhan University, Wuhan, 430072, China

Abstract Many viruses can escape cellular innate antiviral immune responses by encoding one or more proteins to inhibit the induction of type I interferons (IFN-α/β), which leads to the occurrence of major diseases. However, the mechanisms how some virus-encoded proteins inhibit IFN-α/β induction have not yet been fully understood. Based on available literature and experimental data of classical swine fever virus (CSFV), in this study, we develop a mathematical model of virus- and dsRNA-triggered type I IFN signaling pathways, and investigate the quantitative relationship between the dose of the transfected plasmid and the inhibitory effects of N^{pro} or E^{rns}. Our simulation results showed that CSFV N^{pro} inhibited both dsRNA- and virus- induced IFN-β expression, and E^{rns} only inhibited exogenous dsRNA-triggered IFN-β production, which are agreement with experimental data. The dose-dependent inhibition by N^{pro} or E^{rns} was observed when the transfected plasmid was less than 1.5 μg. Furthermore, when the plasmid was more than 1.5 μg, the inhibitory effects of both N^{pro} and E^{rns} can reach maximum. These results provide insight into systems properties and generation of hypotheses for further research.

Keywords Mathematical Model; Signaling pathway; Type I interferons; Virus; dsRNA

1 Introduction

Type I interferons (IFNs), including IFNα and IFNβ, play a central role in the innate antiviral immune defense against all kinds of viruses. Viral infection triggers a series of signaling cascades, which lead to the induction of type I IFNs, however, some viruses evolved multiple escape strategies allowing them to suppress IFN production to counteract the antiviral response of host cells[1,2]. It has been experimentally demonstrated that classical swine fever virus (CSFV), as the causative agent of a highly contagious disease of pigs, can encode two viral proteins N^{pro} and E^{rns} to inhibit the virus- and extracellular dsRNA-mediated IFN-β expression respectively [3-7]. However, the mechanisms that how these viruses inhibit IFN-α/β induction have not yet been fully understood.

The system-level analysis of the IFN related signaling pathways has attracted the attention of many researchers. In recent years, the control mechanism and coordination of IFN-induced JAK-STAT signaling pathways were investigated by employing mathematical modeling and theoretic analysis [8-12]. To our best knowledge, the modeling of signaling pathways that virus-mediate IFN gene

* xfzou@whu.edu.cn

expression has not been reported in the literature. In this study, we develop the mathematical model of dsRNA- and virus-triggered type I IFN signaling pathways and investigate the quantitative relationship of inhibiting IFN-induction by viral proteins.

2 Model and Methods

Previous studies showed the production of IFN-β in response to mimetic poly(IC) that is a synthetic mimetic of viral double-stranded RNA (dsRNA) and virus infection is through distinct signaling pathways, one dependent upon Toll-like receptor 3 (TLR3) and the other dependent on the RNA helicases retinoic acid-inducible gene-I (RIG-I) and melanoma differentiation-associated gene 5 (MDA5)[13,14]. Although TLR3 and RNA helicases interact with different molecules during the proximal signaling events triggered by dsRNA, these two parallel viral recognition mechanisms converge on activation of the transcription factors IRF-3/7, AP-1 and NF-κB, leading to expression of IFN-α/β. According to the available literature and experimental observations of classical swine fever virus (CSFV), we draw the graph of dsRNA- and virus-triggered type I IFNs signaling pathways (Fig.1). The detailed description of the signal transduction processes is presented in Supplementary Section1.

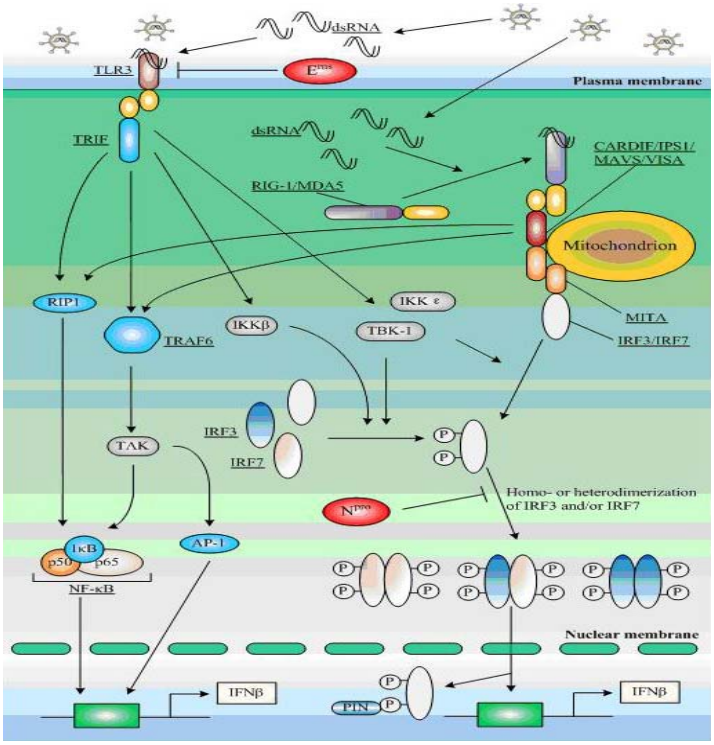

Figure 1: The graphical representation of dsRNA- and virus-triggered type I IFN signaling pathways, including all key components considered in the model.

Due to the complexity of virus-induced signaling pathways, only those components that are involved in interactions and the most important dynamic processes are included in this study. The graphical representation of the mathematical model including all components and reactions considered is depicted in Supplementary Fig.S1. It involves the following fundamental modules: (a) formation and dissociation of protein complexes; (b) protein degradation; (c) phosphorylation and phosphatase activation; (d) gene transcription; (e) mRNA translation; (f) Nuclear import and export of molecules. Because enzyme concentrations are relatively high in the signaling pathways, the condition that the substrate concentration is much larger than the enzyme is not satisfied. Therefore the processes were assumed to follow the mass action law and Michaelis-Menten equation is not used like other literature [8-10]. We describe the dynamics of systems using a set of ordinary differential equations, which are listed in Table 1. In the model, all reactions were divided into 16 types according to their reaction features, and we assumed that reactions in the same type have the same rate constants. Therefore, in the model, there were 88 variables and 28 associated rate constants (See Supplementary Table S1). The initial concentrations (Supplementary Table S2) were set based on the experimental observations and available literature [3,7-9]. All kinetic parameters in the model are fitted to the published and unpublished experimental data[7] by using the genetic algorithm [15, 16](Supplementary Table S3).

Table 1: Kinetic equations in the model

d[m_{dsRNA1}]/dt= - v1, d[m_{dsRNA2}]/dt= -v6, d[m_{TLR3}]/dt=-2v1-v2 ,
d[m_{TRIF}]/dt=-v3, d[m_{TRAF6}]/dt=-v4-v8, d[m_{ikkb}]/dt=-v10(1)
d[m_{ikkε}]/dt=-v11(1)-v22(1)+v22(2) , d[m_{TBK1}]/dt=-v12(1)-v21(1)+v21(2)
d[m_{IRF3}]/dt=-v13(1)-v14(1)-v43, d[m_{IRF7 }]/dt=-v15(1)-v16(1)-v44
d[m_{PIN1}]/dt=-v33-v34-v35, d[m_{RM}]/dt=-v6, d[m_{VISA}]/dt=-v7,
d[m_{RIP1}]/dt=-v9, d[m_{TAK}]/dt=-v17(1)-v23(1), d[m_{NF_kB}]/dt=-v24(1)
d[m_{AP1}]/dt=-v20(1), d[m_{MITA}]/dt=-v36-v37-v39+v41+v42,
d[m_{MITA_IRF3}]/dt=+v37-v38-v50, d[m_{MITA_IRF7}]/dt=+v39-v40-v51
d[m_{Npro}]/dt= $-\sum_{i=43}^{57} vi$, d[m_{Erns}]/dt=-v2
d[m_{mRNAn}]/dt=+v60+v61+v62+v63+v64-v58
d[m_{mRNAc}]/dt=v58-v59-v65, d[m_{IFNβ}]/dt=v59-v66,
d[m_{act_TLR3}]/dt=2v1-v3
d[m_{act_TRIF}]/dt=+v3-v4-v5-v10(1)+v10(2)-v11(1)+v11(2) -v12(1)+v12(2)
d[m_{actT_TRAF6}]/dt=v4-v17(1)+v17(2), d[m_{actT_RIP1}]/dt=v5-v18(1)+v18(2)
d[m_{act_RM}]/dt=v6-v7, d[m_{act_VISA}]/dt=v7-v8-v9-v36
d[m_{actV_TRAF6}]/dt=v8-v23(1)+v23(2), d[m_{actV_RIP1}]/dt=v9-v24(1)+v24(2)
d[m_{_act_TRIF}]/dt=+v10(1)-v10(2)
d[m_{_ikkb}]/dt= +v10(2)-v13(1)+v13(2) -v15(1)+v15(2)
d[m_{ikkε_act_TRIF}]/dt=v11(1)-v11(2), d[m_{act_ikkε}]/dt=v11(2)-v16(1)+v16(2)
d[m_{TBK1_act_TRIF}]/dt=v12(1)-v12(2),

d[m_{act_TBK1}]/dt=v12(2) -v14(1)+v14(2)
d[m_{IRF3_act_ikkb}]/dt=+ v13(1)-v13(2)
d[m_{IRF3P}]/dt=+v13(2)+v14(2)-2v25-v26+v41-v45
d[m_{IRF3_act_TBK1}]/dt= v14(1)-v14(2), d[m_{IRF7_act_ikkb}]/dt=v15(1)-v15(2)
d[m_{IRF7P}]/dt=+v15(2)+v16(2)-2v27-v26+v42-v46
d[m_{IRF7_act_ikkε}]/dt=+ v16(1)-v16(2),
d[m_{TAK_ actT_TRAF6}]/dt=+ v17(1)-v17(2)
d [m_{TAK_actV_TRAF6}]/dt=+ v23(1)-v23(2)
d[m_{act_TAK}]/dt=+v17(2)-v19(1)+v19(2)+v23(2)
d[m_{NF_kB_actT_RIP1}]/dt=v18(1)-v18(2),
d[m_{NF_kB_actV_RIP1}]/dt= v24(1)-v24(2)
d[m_{act_NF_kB}]/dt=+v18(2)+v19(2)+v24(2)-v31
d[m_{NF_kB_act_TAK}]/dt=v19(1)-v19(2), d[m_{AP1_act_TAK}]/dt=v20(1)-v20(2)
d[m_{act_AP1}]/dt=+v20(2)-v32, d[m_{IRF3P2}]/dt=+v25-v28-v47
d[m_{IRF3P_IRF7P}]/dt=+v26-v29-v49, d[m_{IRF7P2}]/dt=+v27-v30-v48
d[m_{IRF3P2n}]/dt=+v28-v33-v60, d[m_{IRF3P_IRF7Pn}]/dt=+v29-v34-v61
d[m_{IRF7P2n}]/dt=+v30-v35-v62, d[m_{act_NF_kBn}]/dt=+v31-v63
d[m_{act_AP1n}]/dt=+v32-v64, d[m_{PIN1_ IRF3P2n}]/dt=+v33
d[m_{PIN1_ IRF3P_IRF7Pn}]/dt=+v34, d[m_{PIN1_ IRF7P2n}]/dt=+v35
d[m_{VISA_MITA}]/dt=+v36-v38-v40+v41+v42
d[m_{VISA_MITA_MITA_IRF3}]/dt=+v38-v21(1)-v52
d[m_{TBK1_VISA_MITA_MITA_IRF3}]/dt=+v21(1)-v21(2)-v54
d[m_{VISA_MITA_MITAP_IRF3}]/dt=+v21(2)-v41-v56
d[m_{VISA_MITA_MITA_IRF7}]/dt=+v40-v22(1)-v53
d[m_{ikkε_VISA_MITA_MITA_IRF7}]/dt=+v22(1)-v22(2)-v55
d[m_{VISA_MITA_MITAP_IRF7}]/dt=+v22(2)-v42-v57
d[m_{Npro_IRF3}]/dt=+v43, d[m_{Npro_IRF7}]/dt=+v44
d[m_{Npro_IRF3P}]/dt=+v45, d[m_{Npro_IRF7P}]/dt=+v46
d[m_{Npro_IRF3P2_ Npro}]/dt=+v47, d[m_{Npro_IRF7P2_ Npro}]/dt=+v48
d[m_{Npro_IRF3P_IRF7P_Npro}]/dt=+v49, d[m_{Npro_MITA_IRF3}]/dt=+v50
d[m_{Npro_MITA_IRF7}]/dt=v51, d[m_{Npro_VISA_MITA_MITA_IRF3}]/dt=+v52
d[m_{Npro_VISA_MITA_MITA_IRF7}]/dt=+v53
d[m_{Npro_TBK_VISA_MITA_MITA_IRF3}]/dt=+v54
d[m_{Npro_ikkε_VISA_MITA_MITA_IRF7}]/dt=+v55
d[m_{Npro_VISA_MITA_MITAP_IRF3}]/dt=+v56
d[m_{Npro_VISA_MITA_MITAP_IRF7}]/dt=+v57 , d[m_{Erns_TLR3}]/dt=+v2

3 Results

3.1 Comparisons between simulation results and experiment data

We use the model to do numerical simulations under the stimulation with poly(IC) or Sendai virus to analyze inhibitory effect of Npro or Erns on signaling pathways. As

seen in Fig.2, our simulation results show that CSFV N^{pro} inhibits both the poly(IC)- and Sendai virus-triggered IFN-β production (Fig.2(a) and Fig.2(c)), and that E^{rns} has only inhibition of poly(IC)-stimulated IFN-β induction in dose-dependent way (Fig.2(d)), but had no influence on Sendai virus-activated IFN-β gene expression (Fig.2(b)), which are consistent with the experimental results which are calculated according to experimental data [7].

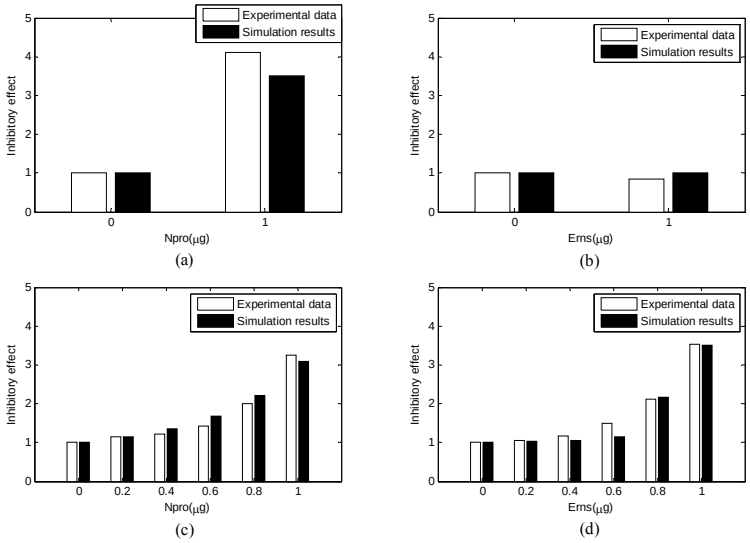

Figure 2: Comparisons between experimental and simulation results of CSFV N^{pro} and E^{rns} for inhibition of virus- and dsRNA-triggered IFN-β production. (a) & (b): Stimulated with Sendai virus; (c) & (d): Stimulated with ploy(IC).

3.2 The inhibitory effects do not exceed a biggest value

To further investigate the maximal dose of CSFV E^{rns} or CSFV N^{pro} plasmid for complete inhibition of IFN-β production, we set up the plasmid dose range from 0 μg to 4 μg at 0.1μg dose interval, and run a separate simulation to check inhibitory effects. The results showed that the inhibitory effects are quickly increasing within the 1μg dose of plasmid, and reached complete inhibition at approximately 1.5μg dose (Fig.3). Ninety percent of the complete inhibition was observed at 1μg dose of single plasmid of two E^{rns} and N^{pro} plasmids. These findings further demonstrated that our experimental data obtained with 1μg single plasmid of two E^{rns} and N^{pro} plasmids are valid and reliable, and represent authentic biological characteristics.

3.3 The transcription factor IRF3P exhibits different feature in dsRNA-triggered signaling pathways

To elucidate mechanism of CSFV N^{pro}- and E^{rns}-mediated inhibition on IFN-β signaling pathways, we simulated the concentration of IRF3P molecule in signaling pathway in cells treated with exogenous dsRNA with N^{pro} or E^{rns} respectively. As an

important transcription factor for virus-triggered induction of type I IFNs, IRF3P was reduced in a dose-dependent manner by both N^{pro} and E^{rns} (Fig. 4). Dissimilarly, N^{pro} reduced only the peak amplitude of IRF3P (Fig. 4a), but E^{rns} decreased the peak amplitude of IRF3P as well as delayed its peak time (Fig. 4b). This is because N^{pro} directly interacted with IRF3 whereas E^{rns} acted as an upstream molecule of TLR3 in the signaling pathway.

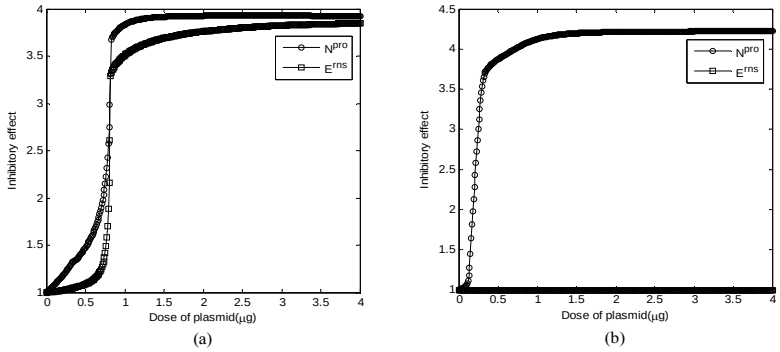

Figure 3: The relationship between the dose of Npro or Erns plasmid and their inhibitory effects. (a): Stimulated by poly(IC); (b): Stimulated by Sendai virus.

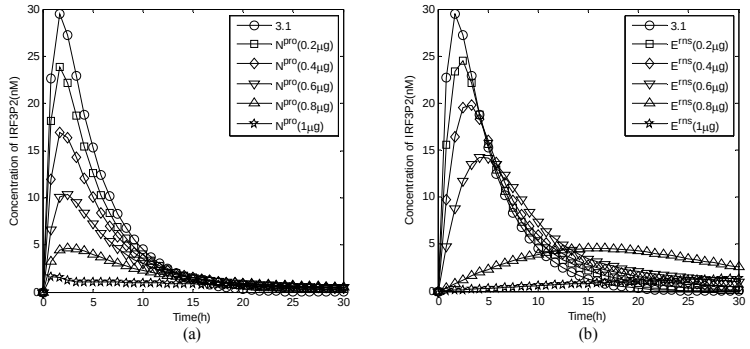

Figure 4: Simulated time course of IRF3 activation in cells stimulated by poly(IC) with (a) pcDNA/N^{pro} and (b) pcDNA/E^{rns}, the legend 3.1 with circle and solid line represents the negative control plasmid pcDNA3.1

4 Sensitivity Analysis of Model Parameters

The sensitivity analysis of model parameters is very important to understand how certain properties of the model depend on the choice of parameter values. To check this, all parameters were randomly changed under the range of -10% to +10% and a separate simulation was run. 100 sets of parameters have been tested and Fig.5 indicated that the model response was robust with respect to perturbation of parameters.

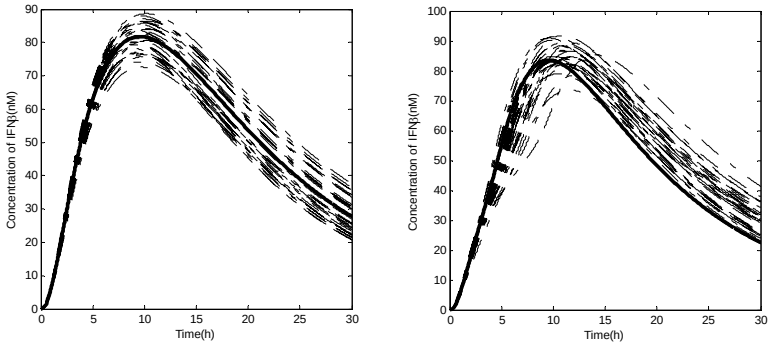

Figure 5: Model sensitivity to parameter changes: the time course of IFNβ when the cell is stimulated by (a) poly(IC) and (b) Sendai virus. The real line and dashed line represent the time course of IFNβ with parameters listed at Table S3 and parameters after perturbation, respectively.

5 Discussion and Conclusions

IFN-α/β represent one of the first lines of defense of the innate immune system and their role in the pathogenesis of autoimmunity remains at the forefront of scientific inquiry[17]. It is greatly significant to understand the complex mechanism of virus-inhibited IFN-α/β induction by means of systems-level analyses of signaling pathway behavior. In the present study, based on available literature and biological experimental data of CSFV, we presented for the first time a mathematical model for the dynamics of virus-stimulated type I IFN signaling pathways. The consistency between simulation results and experiment data indicated that our model is reasonable. We used the model to identify the different influence of N^{pro} and E^{rns} on signaling pathways. The results of the quantitative analysis also showed that inhibitory effects are dependent on the dose of plasmid but it can reach maximum when the dose of plasmid is approximately 1.5μg. This can reasonably explain why 1μg plasmid or no more than 2μg was used in most of related experiments.

Acknowledgements

This work was supported by Chinese National Natural Science Foundation grants No. 30670083 and 30771597

Supplementary Materials

Supplementary materials are available at
http://maths.whu.edu.cn/jsgrzy/zxf/paper/supplements.PDF

References

[1] Weber F., Kochs G., Haller O., Inverse Interference: How Viruses Fight the Interferon System, *Viral Immunology*,17(4), 498-515,2004.

[2] Haller O., Kochs G., Weber F.: The interferon response circuit: induction and suppression by pathogenic viruses, *Virology*, 344, 119-130, 2006.

[3] Bauhofer, O., Summerfield, A., Sakoda, Y., Tratschin, J.D., Hofmann, M.A. and Ruggli, N. , Classical swine fever virus Npro interacts with interferon regulatory factor 3 and induces its proteasomal degradation, *J Virol*, 81, 3087-3096, 2007.
[4] La Rocca S.A., Herbert R.J., Crooke H., Drew T.W., Wileman T.E. and Powell P.P., Loss of interferon regulatory factor 3 in cells infected with classical swine fever virus involves the N-terminal protease, Npro, *J Virol*, 79, 7239-7247, 2005.
[5] Ruggli N., Tratschin J.D., Schweizer M., McCullough K.C., Hofmann M.A. and Summerfield A., Classical swine fever virus interferes with cellular antiviral defense: evidence for a novel function of N(pro), *J Virol*, 77, 7645-7654, 2003.
[6] Seago J., Hilton L., Reid E., Doceul V., Jeyatheesan J., Moganeradj K., McCauley J., Charleston, B. and Goodbourn, S., The Npro product of classical swine fever virus and bovine viral diarrhea virus uses a conserved mechanism to target interferon regulatory factor-3, *J Gen Virol*, 88, 3002-3006, 2007.
[7] Luo X., Ling D, Li T, Wan C, Zhang C, Pan Z. , Classical swine fever virus Erns glycoprotein antagonizes induction of Beta interferon by double-stranded RNA. *Canadian Journal of Microbiology*, 2009 (In press).
[8] Smieja A., Jamaluddin M., Brasier A.R. and Kimel M., Model-based analysis of interferon-β induced signaling pathway, *Bionformatics*, 24, 2363–2369, 2008.
[9] Yamada S., Shiono S., Joo A., Yoshimur A., Control mechanism of JAK/STAT signal transduction pathway, *FEBS Letters*, 534, 190-196, 2003.
[10] Zi Z., Cho K.H., Sung M.H., Xia X., Zheng J. and Sun Z. , In silico identification of the key components and steps in IFN-gamma induced JAK-STAT signaling pathway, *FEBS Lett*, 579, 1101-1108, 2005.
[11] Beirer S. and Hofer T., Control of signal transduction cycles: general results and application to the Jak-Stat pathway, *Genome Inform*, 17, 152-162, 2006.
[12] Soebiyanto R.P., Sreenath S.N., Qu C.K., Loparo K.A. and Bunting K.D., Complex systems biology approach to understanding coordination of JAK-STAT signaling, *Biosystems*, 90, 830-842, 2007.
[13] Li K., Chen Z.H., Kato N., Gale M.J., and Lemon S.M., Distinct Poly(I-C) and Virus-activated Signaling Pathways Leading to Interferon-β Production in Hepatocytes, *THE Journal of Biological Chemistry* , 280,16739–16747, 2005.
[14] Haller O., Kochs G. and Weber F., The interferon response circuit: induction and suppression by pathogenic viruses, *Virology*, 344, 119-130, 2006.
[15] Chan K.Y. and Fogarty T.C. ,2003, Experimental Design Based Multi-parent Crossover Operator, Lecture Notes in Computer Science, Vol. 2610, Springer Berlin / Heidelberg,583-588.
[16] Eiben A.E., Kemenade H. M., Diagonal crossover in genetic algorithms for numerical optimization, *Journal of Control and Cybernetics*, 26 (3), pp. 447–465, 1997.
[17] Theofilopoulos A.N., Baccala R., Beutler B., and Kono D. H., Type I Interferons (α/β) in Immunity and Autoimmunity, *Annual Review of Immunology*, 23, 307-335, 2005.